JOURNAL OF GAS TECHNOLOGY

Volume 8 /Issue 2 / Winter 2023 / Pages 35-55

Journal Home page: http://jgt.irangi.org

Simulation and Economic Evaluation of Flare Gas Recovery Using Nano Adsorbents

Meisam Bijanikhooy[1], Zohreh Saadati[2*], Afsaneh Maleki[2]

1. Ph.D. Student, Department of Chemistry, Omidiyeh Branch, Islamic Azad University, Omidiyeh, Iran
2. Associate Professor, Department of Chemistry, Omidiyeh Branch, Islamic Azad University, Omidiyeh, Iran

ARTICLE INFO

ORIGINAL RESEARCH ARTICLE

Article History:
Received: 15 October 2023
Revised: 16 November 2023
Accepted: 06 December 2023

Keywords:
Sorbent
Silica gel
Molecular sieve
Flare simulation
Natural gas

ABSTRACT

The oil and gas industry is facing a critical challenge with the growing emissions of flare gases, driven by the global expansion of the industry and increased fossil fuel consumption in refineries and petrochemical plants. The significant environmental impact of these flare gas emissions has created a pressing need to develop effective strategies to minimize the associated environmental risks. However, implementing technologies to reduce flare gas emissions presents both economic and environmental hurdles.

In this study, we investigated the application of nanoadsorbents in packed bed towers as a promising approach to recover and repurpose flare gases. Using MATLAB software, we conducted two case studies to evaluate the performance of different adsorbent materials, including Ws and H silica gels, as well as a 4 $\AA$ molecular sieve, for the recovery and conversion of sour flare gas into sweet, moist gas. The analysis revealed that the Langmuir isotherm model provided the most suitable simulation results, demonstrating the technical feasibility and effectiveness of this approach.

DOR: 20.1001.1/jgt.2024.2025628.1037

How to cite this article
M. Bijanikhooy, Z. Saadati, A. Maleki, Simulation and Economic Evaluation of Flare Gas Recovery Using Nano Adsorbents. Journal of Gas Technology. 2023; 8(2): 35-55. (https://jgt.irangi.org/article_714871.html)

* Corresponding author.
E-mail address: zo.saadati@iau.ac.ir, (Z. Saadati).

Available online 31 December 2023

1. Introduction

Petrochemical and oil & gas industries commonly use flaring stacks to burn flammable gas components, which is an unavoidable process for pressure control and safety management. However, gas flaring has become one of the most critical energy and environmental issues worldwide, resulting in environmental consequences and intense health issues for local populations (Mirrezaei and Orkomi, 2020). Flare gas production is particularly high in countries such as Russia, Nigeria, and Iran, which account for a significant portion of the total volume of gasses burned globally. Additionally, gas flaring causes energy loss and economic costs in countries. While waste hydrocarbon gasses contain valuable compounds such as methane, natural gas, and ethylene that have significant economic value, the proper disposal of these gasses is still one of the most pressing environmental problems in the oil, gas, and petrochemical industries (Soltanieh 2016, Bank 2004, Anejionu 2015). (Table 1) shows the amount of flare gas production from 2007 to 2011 in different countries, highlighting the increase in flare gas production in the United States from 2.2 billion m^3 in 2007 to 7.1 billion m^3 in 2011(Davoudi 2013).

Table 1. The Amount of Flare Gas Production from 2007 to 2011 in the Different Countries

Year	2007	2008	2009	2010	2011	Changes from 2010 to 2011
Russia	52.3	42	46.6	35.6	37.4	1.8
Nigeria	16.3	15.5	14.9	15	14.6	-0.3
Iran	10.7	10.8	10.9	11.3	11.4	0.1
Iraq	6.7	7.1	8.1	9	9.4	0.3
America	2.2	2.4	3.3	4.6	7.1	2.5
Algeria	5.6	6.2	4.9	5.3	5	-0.3
Kazakhstan	5.5	5.4	5	3.8	4.7	0.9
Angola	3.5	3.5	3.4	4.1	4.1	0
Saudi Arabia	3.9	93	3.6	3.6	3.7	0.1
Venezuela	2.2	2.7	2.8	2.8	3.5	0.7
All the first 20 countries	132	124	127	118	121	3.1
Other parts of the world	22	22	20	20	19	-1.1
The whole world	154	146	147	138	140	1.9

Flare gas burning has negative consequences on the ecosystem as well. Economic loss is another outcomes. According to estimates, the value of the gases flared globally in 2019 was $30.6 billion,or 30% of the gas consumed by EU (Tofigh and Abedian, 2016). To address this issue, the World Bank initiative "Zero routine flaring by 2030" aims to eliminate routine gas flaring and reduce the environmental impact of flare gasses. There are numerous approaches to decrease gas flaring, but they will probably call for fresh ways to gas monetization, incentives and business plans. A growing number of businesses have pledged to do away with flaring by 2030 (Mansoor and Tahir, 2021). By 2030, all non-emergency and wasteful flaring must be stopped in order to reach the net-zero flaring plan by 2050, this will allow for

the reduction or elimination of 90% of flare gasses by that time. One alternative to reduce flaring is the use of flare gas recovery (FGR) systems, which recover flammable gas for reuse as fuel for process heaters. The FGR system is a new technique applicable to refining waste that reduces the continuous flare operation, decreasing thermal radiation, associated smoke, noise, and pollutant emissions related to flaring (Bank 2004). Numerous researches indicate that this process and its usage are promising economically (Heydari, 2016, Hajizadeh 2018 Barekat-Rezaei 2018, Romsom and McPhail, 2021, Jafari 2021, Sabaghian 2022). However, the collection and exploitation of flare gasses have limitations that oil and gas-producing countries are facing, making performance optimization and modification of this part of the oil and gas industry crucial (Ahsan 2019). In this case, unfortunately, because of the high cost of recovery infrastructures, technical challenges, and a lack of suitable policies and regulatory frameworks prior to such commericial endeavors, flare gas recovery in Iran is still in its infancy (Barati 2019).

In a study in 2012, Rahimpour and Jokar discussed the technical feasibility of flare gas conversion and its use in the Farashband gas refinery using a simulation model. They concluded that electricity generation from Aghar and Dalan gas fields is economical (Rahimpour 2012).

In 2015, Wallace investigated the Bacon Formation as the world's largest shale reservoir. Its studies led him to the conclusion that flare gases can be applied to fuel drilling rigs during drilling operations (Wallace 2015).

In another work conducted in 2015, three approaches to flare gas reduction were suggested. These included injection gas into; South Pars reservoir, the feed stream of South Pars gas refineries, and Aghajari oil field. From an operational perspective, gas compression and injection into the fifth national pipeline was the best course of action. The outcomes showed that flare gas could be recovered at a high ratio and that gas transmission capacity could be increased (Hashemi Fard and Shafiee, 2019).

In 2016, Adekomaya et al, in a conducted resaearch stated that 42.6% of the extracted gas in Nigeria is flared daily, which can be used in thermal power plants, and the failure to supply electricity is the result of the lack of gas for power plants. They stated that by using flare gas, they will reach a sustainable level in the production and distribution of electricity (Adekomaya 2016).

In a different study conducted in 2016, Khanipour investigated the recovery of gas from flare gas and its subsequent reintroduction to the methanol synthesis reactor. According to the modelling data, there was an increase in methanol production with the returned gas. Furthermore, the analysis and simulation of important gas separation parameters revealed the ultrahigh ratio separation of recovered gases (khanipour 2016).

In 2019, Ojiagwo et al in a work examined the use of gas technology as an option to minimize gas degassing in Nigeria and minimize its environmental impact. The results of this study showed that electricity production through the use of part of the annual 18.27 BCM of gas in Nigeria will improve from its current daily production of 4358 MW to about 12000 MW. This serves as fuel for 50 gas turbine units with an output power of 150 MW each, with a potential increase in daily power generation of 7,500 MW.20 (Ojiagwo 2019).

Recent studies have focused on the recovery of valuable compounds from gas sent to the flare using a membrane or simulation model. For instance, In 2017, the economic investigation and technical characterization of FGR in different gas processing plants were examined in a research by Zolfaghari. Aspen HYSYS has been used to simulate three different process: GTL, gas turbines generation (GTG), and gas to ethylene (GTE). The outcomes demonstrated

how profitable these techniques are very year and how economical they are (Zolfaghari 2017).

In 2018, the integrated flare gas to gasoline (FGTG) process was studied by Jafari through technical analysis and simulation. In this work the Aspen HYSYS software was used to simulate integrated FGTG process for turning flare gas to gasoline. The simulation findings showed that gasoline may be raised by an average of 55% and 10% respectively, by recycling all gas emissions back into the process, including off gas from the methanol and MTG units (Jafari 2018).

in 2019 in a study, Saeedi et al estimated the use of catalytic membrane reactor as a new approach for gas recovery. In this research a comprehensive two-dimensional non-isothermal model was developed to evaluate the performance of gas recovery process with flame in membrane reactor. The environmental investigation showed that by using the catalytic membrane reactor to recover the greenhouse gases of Assalouye gas processing plant (Iran), the equivalent volume of greenhouse gas emission was reduced considereably (Saidi 2019).

Another study by Zhao et al. in 2021 proposed a novel approach to recover natural gas liquids (NGLs) from flare gas using a membrane separation process. The study demonstrated that the proposed membrane-based NGL recovery process can achieve high NGL recovery rates with low energy consumption (Zhao 2021).

In 2021 in a similar work by Jafari, design, simulation and economic investigation the process of DME (turning flare gas to dimethyl ether) in order to the production of gasoline, LPG (Liquefied petroleum gas) and hydrogen were conducted by Aspen HYSYS v.11 software, which the results were very promising (Jafari 2021).

In 2022, in a project by Sabaghian, the perspective use of the separated CO_2 from the flare gas in Parsian refinery for injection into a gas condensate reservoir was studied, which the results were very desirable (Sabaghian 2022).

To sum up, gas flaring contributes significantly to greenhouse gas emissions that contaminate the environment (Deljoo 2023). Nevertheles, there are precious compunds whith substantial economic worth found in the waste hydrocarbon gases from industrial units and complexes. Therefore, it is crucial to recognize alternatives for decreasing the flaring of these components by reusing and recovering this resource (Ng 2023). One option for reducing flaring is the use of FGR systems, and optimizing the oil and gas industry is essential in this regard. Several Studies have investigated the recovery of valuable compounds from the gas sent to the flare using a membrane or simulation models (Deljoo 2023).

The current project investigates the recovery of flare gases using nanoadsorbents to remove harmful compounds and assesses the technical and economic aspects of flare gas recovery from natural gas resources. The use of silica gel Ws, silica gel H, and molecular sieve 4 $\mathring{A}$ for dehumidification and sweetening of flare gas is explored to recover these valuable gases for different purposes contributing to increased national income. MATLAB software is used to model and simulate adsorption systems with nano-adsorbers, optimize the flaring system of two refineries as case studies, and evaluate the economic benefits of adsorption towers filled with nano-adsorbents as an alternative to flaring. The Parsian gas refinery, which is the third largest refinery in Iran and a significant supplier of the country's energy, was chosen as the first case study. The characteristics of the input and output gasses of the adsorption towers are presented, indicating the potential for recovery. The twelfth phase of South Pars with the most input gas flow and the highest volume of gas sent to flare is chosen as the second case study, highlighting the importance of recovering these gasses for economic gain and preventing environmental damage. The project findings provide valuable insights into reducing flare gas emissions and utilizing these valuable resources, indicating the novelty and importance of this work in contributing to Iran's

economic growth and sustainability.

2. Methodology

In this study, we investigated the use of MATLAB software to model and simulate adsorption systems with nanoadsorbers. We also conducted case studies to optimize the flaring systems of two refineries. For the first case study we conducted simulations and modeling using the isotherms of Langmuir and LAST. We then compared and evaluated the simulation outcomes with experimental results. For the second case study we used an appropriate isotherm model with modified modeling and examined the results of the simulation under different operating conditions. We also evaluated the economic feasibility of using adsorption towers filled with nanoadsorbents as an alternative to flare. The simulations were performed using the powerful MATLAB software, and the project was evaluated based on the simulation results.

As the first case study, we examined the Parsian gas refinery, as the third largest refinery in Iran which has a daily production capacity of 82 Mm^3 of natural gas and supplies 10% of the country's energy. In this complex, after separation processes in floodgates and separator containers, natural gas is dehumidified and the dew point is adjusted before being injected into the fourth nationwide line. The temperature of the gas entering the adsorption tower is 35-45 ℃ in summer and 25-30 ℃ in winter, and the dry gas comes out from the bottom of the tower after passing through a filter. The refinery has four towers that are used to adjust the dew point, with two towers for adsorption and the others for cooling and heating. The adsorption towers are placed in a specific order in the circuit, and the maximum pressure drop along the length of the tower is 0.7 according to the tower design. (Table 2) presents the input and output gas characteristics of the towers.

As our project focused on the recovery of flare gas, we chose the ninth refinery or the twelfth phase of South Pars for investigation. This was due to the fact this refinery currently has the highest input gas flow, which this means it sends the highest gas volume to the flare. Recovering these gases can have a positive impact on the economy and prevent irreparable damage to the environment. (Tables 3, 4, & 5) provide the characteristics of the sent gas to the flare during normal operating mode.

During the full operation mode, this refinery injects 3 Mft^3 of sour gas (equivalent to 75 Mm^3 of sweet gas) into the national network daily. Additionally, this phase produces 120 thousand barrels of gas condensate and 750 tons of sulfur for export. With the inclusion of this phase in the production circuit as well as the increase in Iran's gas contribution from the world's largest gas field, the country's gross national product is expected to increase by three percent, leading to a fundamental change in the national economy. This underscores the importance of the twelfth phase of South Pars (Keshavarz 1394).

Table 2. The Characterization of the Input and Output gases of Towers are Presented

No	Characteristic	Unit	Input amounts	Output amounts
1	Gas temperature	℃	34.3	37
2	Ws packed-tower height	m	0.64	0.64
3	H packed-tower height	m	6.36	6.36
4	Gas pressure	Bar	90	≈89.3
5	Water molar fraction in gas (Y_A)	--	0.00084	0.00080
6	C_5^+ molar fraction in gas (Y_C)	--	0.00498	0.0030

Table 3. Specifications of the Gas Components Sent to the Flare

No	Components	Molar percentage
1	H_2O	1.746
2	Nitrogen	0.607
3	Carbon Dioxide	10.549
4	H_2S	5.699
5	Methane	41.867
6	Ethane	8.346
7	Propane	5.983
8	i-Butane	1.812
9	n-Butane	3.544
10	i-Pentane	3.500
11	n-Pentane	3.428
12	C6	3.011
13	C7	3.089
14	C8	3.540
15	C9	3.377
	Total	100

Table 4. Specifications of the Gas Flow Rate Sent to the Flare

Parameter	Unit	Value
Flow	$Kg.h^{-1}$	76880
Temperature	°C	50
Pressure	Barg	7.0
Molecular weight	g/mol	40.08

Table 5. Characteristics of the Gas Entering the Circuit

Item	Unit	Value
Water molar fraction	%	0.19
CO_2 molar fraction	%	0.01019
Heavy hydrocarbon molar fraction	%	0.089
Temperature	°C	65
Pressure	Barg	5

3. Results and Discussion

3.1. Modelling of Moisture Adsorbent Tower with Silica Gel

In this study, we developed a model for the adsorption of water and heavy hydrocarbons in Ws and H silica gel, respectively. Due to the low concentrations of these two components in the inlet gas, only the adsorption of these components was considered. A mass transfer equation was written for the adsorbed component in the bed, and Langmuir and IAST models were used to communicate gas-solid equilibrium data. To account for the exothermic process, energy balance equations were used for non-isothermal substrate. Heat transfer in the radial direction was neglected due to the insulation of the walls of the adsorption tower. The system was not isothermal along the length of the tower, so the equations were solved element to element for the calculation of the equilibrium concentration. Mass transfer inside particles was diffusion and outside the bed medium was convection. Langmuir and IAST models were used to compare the results obtained in modeling and the most suitable model was selected. Surface adsorption was applied as a single layer on an ideal surface (Hajizadeh 2019). For the modeling of the adsorbent bed, several assumptions were made, including the same size of adsorbent grains, constant transfer coefficients, constant velocity along the tower, constant overall mass transfer coefficients independent of pressure changes, and a plug flow pattern with axial dispersion. Additionally, only heavy hydrocarbon particles were adsorbed in the H silica gel bed, and only water molecules were adsorbed in the Ws silica gel bed (Gholami 2010). (Figure 1) shows the selective element of silica hemadsorption substrate.

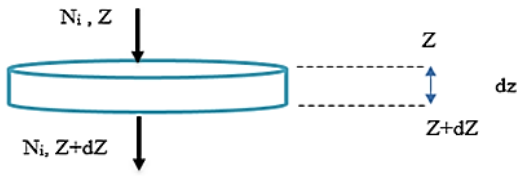

Figure 1. Selective Element of Silica Gel Adsorption Substrate

The considered assumptions for the modeling of the adsorbent bed:

- The same size is assumed for adsorbent grains.
- The transfer coefficients are considered constant.
- Velocity along the tower is considered constant.
- The overall mass transfer coefficients are considered constant and independent of pressure changes.
- The plug flow pattern with axial dispersion is considered.
- In the H silica gel bed, only heavy hydrocarbon particles are adsorbed.
- Only water molecules are adsorbed in the Ws silica gel bed.

The overall mass balance equation is as follows:

$$Input+Output+Generation - Consumption=Accumulation \quad (1)$$

The balance of water component (first part) mass transfer on the surface of Ws silica gel is presented by Eqs. (2) & (3).

$$-Dl\frac{\partial^2 C_1}{\partial z^2}+u\frac{\partial C_1}{\partial z}+\frac{\partial C_1}{\partial z}+\frac{nVp}{\varepsilon\Delta z}\left[\frac{\partial q_1}{\partial t}\right]=0 \quad (2)$$

The volume of adsorbent particles/the void volume of bed:

$$\frac{nVp}{\varepsilon\Delta z}=\frac{Vt-\varepsilon Vt}{\varepsilon Vt}=\frac{1-\varepsilon}{\varepsilon} \quad (3)$$

Integrating Eqs. (2) & (3) will have the following:

$$-Dl\frac{\partial^2 C_1}{\partial z^2}+u\frac{\partial C_1}{\partial z}+\frac{\partial C_1}{\partial z}+\frac{1-\varepsilon}{\varepsilon}\left[\frac{\partial q_1}{\partial t}\right]=0 \quad (4)$$

Eq.(4) shows the concentration change along the bed and time.

The basic conditions for mass balance in Eq.(4) are:

The water vapor concentration in the solid phase is zero Eq. (5). The initial concentration of water vapor in the gas phase is presented in Eq.(6).

Also, the boundary condition for mass balance in Eq. (4) is in accordance with Eqs. (7) & (8).

$$(q_A)_{t=0}=0 \quad (5)$$

$$(C_A)_{t=0}=C_{A0} \quad (6)$$

$$Z=0,\ C_A=C_{A0} \quad (7)$$

$$\mathrm{Z=L},\ (\frac{\partial C_A}{\partial Z})=0 \quad (8)$$

The mass transfer rate for the adsorbed components was calculated by the linear driving force model. In Eq. (8), concentration alteration in the adsorbed phase is proportional to the rate of mass transfer into the particles. Also, only one component (water vapor) is adsorbed by the adsorbent.

$$\frac{\partial q_A}{\partial t}=K_A(q_A^*-q_A) \quad (9)$$

Where K_A is the mass transfer coefficient and q_A^* is the equilibrium concentration in solid and gas phase interface.

The equation of Langmuir and Freundlich isotherm is as follows (Freundlich 1926):

$$\frac{q_A}{q_A^*}=\frac{B_0\exp(\Delta H)P_A}{1+B_0\exp(\Delta H)P_A},\ P_A=P_t\times V_A \quad (10)$$

The adsorption equation of ISTA is shown in Eq. (11).

$$\frac{q_A}{q_A^*}=a\times PA_n^1,\ P_A=P_t\times V_A \quad (11)$$

3.2. Heat Transfer Balance for Water Component (the First Component) in Silica Gel Bed

By simplifying Eq. (1) for energy transfer in the gas phase and simplifying it, the following equation is obtained:

(12)

$$\lambda_L.\frac{\partial^2 T}{\partial x^2}+\rho_g.C_{pg}.u\frac{dT}{dZ}+\rho_s.\frac{(1-\varepsilon)}{\varepsilon}C_{ps}.\frac{dT_s}{dt}+\rho_s.C_{pg}.\frac{dT}{dt}$$

$$=\rho_s.\frac{(1-\varepsilon)}{\varepsilon}\sum_{k=0}^{n}(-\Delta H).\frac{dq1}{dt}+\frac{4h_w}{\varepsilon d}.(T_f-T_w)$$

The energy balance for the solid phase is:

$$\rho_s C_{ps} \frac{dTs}{dt} + \rho(1-\varepsilon_p)\sum_{i=0}^{n=c}(-\Delta H).\frac{dq_1}{dt} = \frac{2h_p}{R_p}(T_f - T_s) \quad (13)$$

The initial conditions were as follows:

$t = 0,\ T(z,0) = T_{0,1}$

$t = 0,\ T_s(z,0) = T_{0,s}$

$t = 0,\ T_f(z,0) = T_{0,f}$

Also, the boundary conditions for energy balance are as Eqs. (14) & (15):

$$Z = L, T_{(L,t)} = T_{Out\ in\ layer\ 1} \quad (14)$$

$$Z = L,\ \frac{dT}{dz}(Z = L) = 0 \quad (15)$$

3.3. Momentum Balance for the Water Component (the First component) in the Silica Gel bed *Ws*

Due to the small pressure drop along the length of the tower, the momentum balance and Organ's equation were ignored.

3.4. The Modeling of Heavy Hydrocarbon Absorber Tower with Silica Gel *H*

Since the system of adsorption of humidity and heavy hydrocarbons is the same, the modeling of the heavy hydrocarbon adsorbent tower is completely similar to that of water vapor removal. However, values such as adsorption coefficients, and mass transfer, related to heavy hydrocarbons replace water vapor in modeling.

3.5. Describing the Numerical Solution of the Above Equations in MATLAB Software

According to the conditions and assumptions included in each section (gas phase and the solid phase in the adsorbent bed), after driving the model for the process in the both sections, differential equations were obtained for each component. In order to obtain the numerical solution of differential equations obtained from modeling in MATLAB software, the explicit finite difference method is used.

3.6. Explaining the Numerical Solution of Different Parts in MATLAB Software Side of Gas Phase

The differential equation obtained for each component is a PDE. To solve the PDE of each component, a finite difference numerical method of pure explicit type was used. The implementation process was as follows: along the length and in middle points in the center with second-order error, in the center of the bed as forward with first-order error, and at the end of the bed as backward with first-order error. To determine the number of steps along the length of the bed, PDE was opened numerically, and the concentration coefficient was obtained in the desired step. Then, considering the number of 100 steps toward the length and observing the condition of stability in such a way that the concentration coefficient becomes positive, the number of steps toward the length of the tower was determined.

3.7. The Contact Surface with the Adsorbent

Since the Langmuir and Freundlich isotherm was chosen for the model, the concentration amount in the first step was obtained in the radius direction and in all steps obtained along the length using the Langmuir-Freundlich equations. In the following, in each specific longitudinal step considering the molar flux from the gas phase side, the concentrations in the longitudinal direction were obtained according to the relationship of the isotherms.

3.8. Modelling

As in the input data, two case studies were investigated. In the modeling must be each two case studies investigated separately. In the first case study, two Langmuir and IAST isotherm models were simulated, which will be discussed.

3.9. The Simulation of the First Part (the First Case Study)

Considering that the case study data is based on the mole fraction of water vapor and

heavy hydrocarbons as well as the inlet and outlet gas temperature, for better comparison and evaluation, the graphs extracted from the simulation are provided based on the mole fraction and gas temperature. On the other hand, since the adsorption system is unstable, for better evaluation and optimization of the process, simulation has also been reported in 4 different periods (15, 30, 45 and 60 min).

First, the outcomes of the simulation by the Langmuir isotherm model are explained. On the other hand, according to the selected explicit finite difference method in the numerical solution of the obtained equations from the modeling the results of the simulation in the MATLAB software are as follows.

3.10. Simulation Based on Langmuir Isotherm

(Figure 2) shows the molar fraction of water vapor along the length of the bed filled with silica gel Ws in the period of 30 min after the beginning of the process. Water vapor molecules are adsorbed by silica gel Ws along the bed and their concentration decreases. As can be seen in (Figure 2), the mole fraction of water vapor output is very close to the actual data from the refinery.

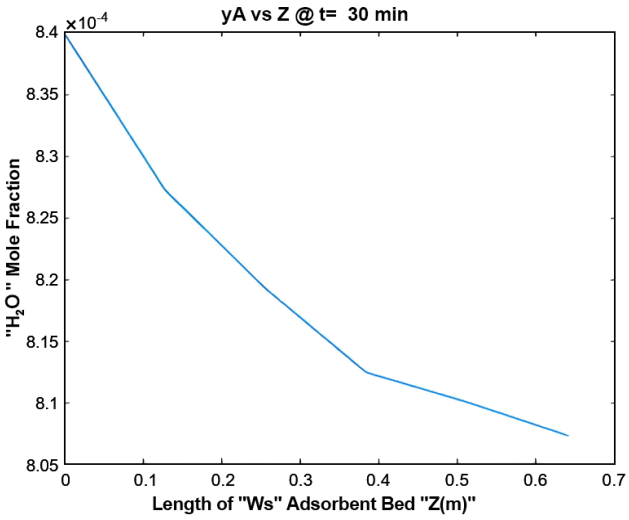

Figure 2. The Mole Fraction of Water Vapor along the Silica Gel bed Ws in Langmuir Model

(Figure 3) shows the molar fraction of C_5^+ along the length of the bed filled with silica gel H in the period of 30 min after the start of the process. C_5^+ molecules are adsorbed by silica gel H along the substrate and their concentration decreases. As can be seen from the (Figure 3), the molar fraction of C_5^+ output is very close to the actual data from the refinery.

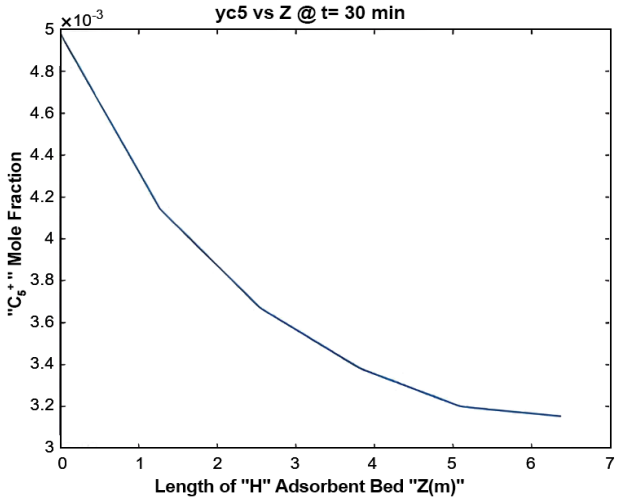

Figure 3. C_5^+ Mole Fraction along the Silica Gel Substrate H in Langmuir Model

According to (Figures 4 & 5), and this fact that the surface adsorption process is exothermic and as well as considering the insulation of the outer surface of the filled bed, the temperature of the gas will be increased along the bed. The temperature increasing trend is more intense in the early stages of the bed length due to more surface adsorption resulted from the large concentration difference in the gas and solid phases. By passing through the final stages of the substrate, the temperature increase is reduced.

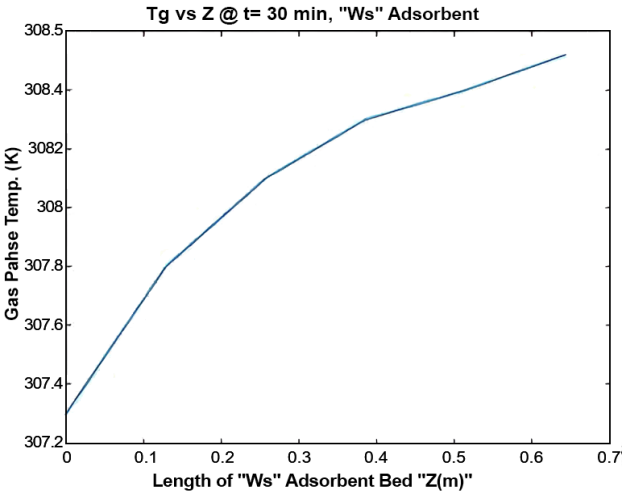

Figure 4. Gas-phase Temperature along the Silica Gel bed Ws in Langmuir Model

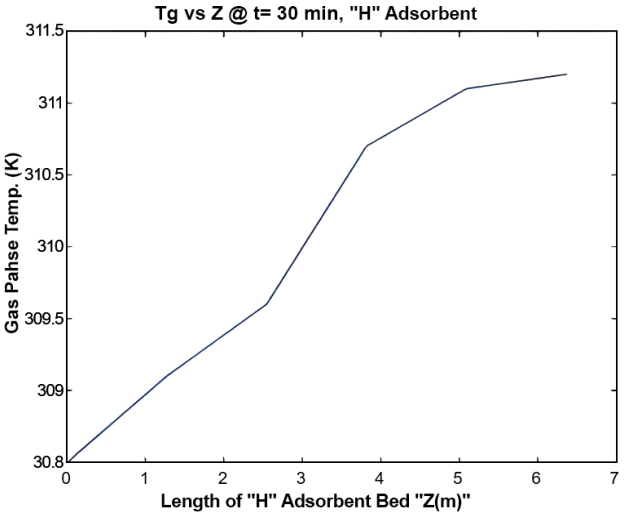

Figure 5. Gas-phase Temperature along the Silica Gel bed H in Langmuir Model

Owing to the instability of adsorption process, the amount of water molecule adsorption was checked in four periods for better evaluation. The outcomes can be seen as shown in the (Figure 5). As can be understood from (Figure 6), due to the concentration polarization difference in the solid and gas phase, the adsorption process in the early times is more, (do not saturation of silica gel with absorbable molecules). Then, over time, based on the saturation of the solid phase, the adsorption process progresses slowly and the filled tower must be entered the reviving stage. As can be seen from the above graphs, the best time to move to reviving stage is between 30 and 60 min.

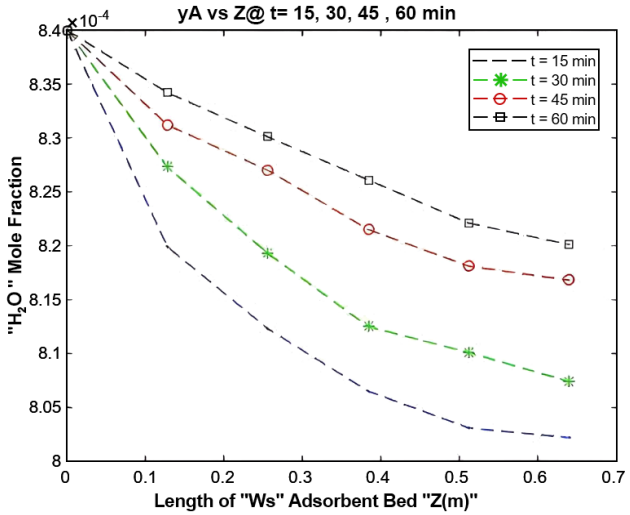

Figure 6. Water Vapor Molar Fraction along the Length of Silica Gel bed Ws in the Langmuir Model in Four Periods

Due to the instability of the adsorption process, the amount of adsorption of C_5^+ molecules was checked in four time periods for better evaluation, and the results can be seen as shown in (Figure 7).

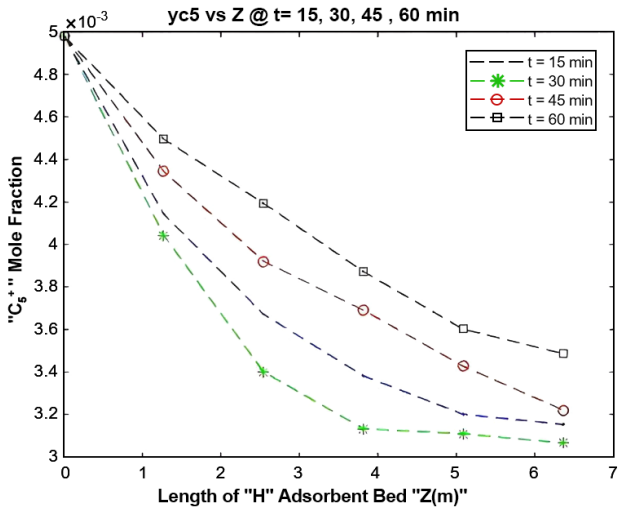

Figure 7. The Mole Fraction (C_5^+) along the Length of Silica Gel bed H in Langmuir Model in Four Time Intervals

As can be understood from the (Figure 7), the adsorption process is higher in the early times due to the concentration potential difference in the solid and gas phase (unsaturation of silica gel from absorbable molecules). Then, over time, based on the saturation of the solid phase, the adsorption process progresses slowly and the filled tower must be entered the regeneration stage. As can be seen from the above charts, the best time to move to the resuscitation stage is between 30 and 60 min.

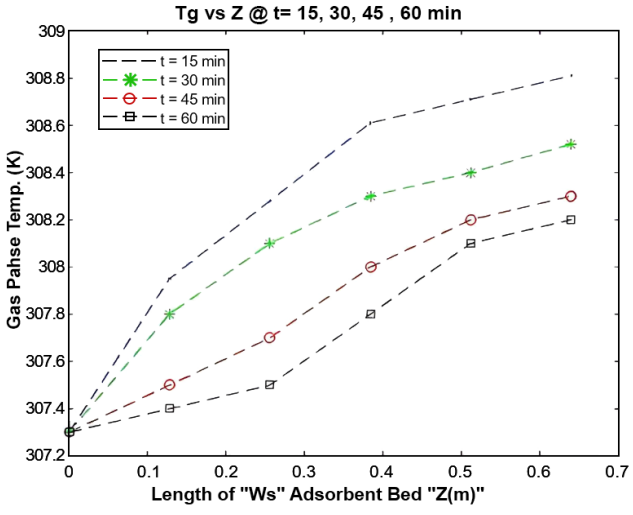

Figure 8. The Temperature of the Gas Phase along the Length of the Silica Gel bed Ws in Langmuir Model in Four Time Intervals

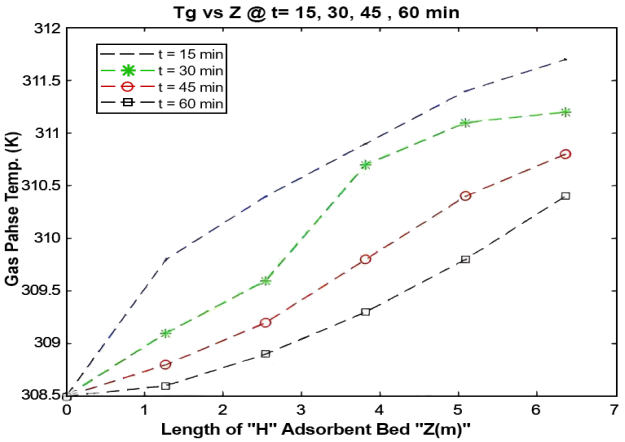

Figure 9. The Temperature of the Gas Phase along the Length of the Silica Gel bed H in the Langmuir Model at Four Time Intervals

According to (Figures 8 & 9), the temperature of the gas fluid experiences a lower temperature increasing over time along the bed, which the reason for this happening is the high concentration potential difference in the early times as explained earlier. Moreover, the saturation of the adsorbent bed with desired molecules over the time is another reason for this.

3.11. The Simulation Based on the IAST Isotherm Model

The above graph (Figure 10) shows the mole fraction of water vapor along the length of the bed filled with silica gel Ws for 30 minutes after the start of the process. Water vapor molecules are adsorbed by silica gel Ws along the bed and their concentration are decreased. As can be seen from the (Figure 9), the mole fraction of water vapor output is far from the actual data from the refinery, which this indicates the inadequacy of this isotherm in this system.

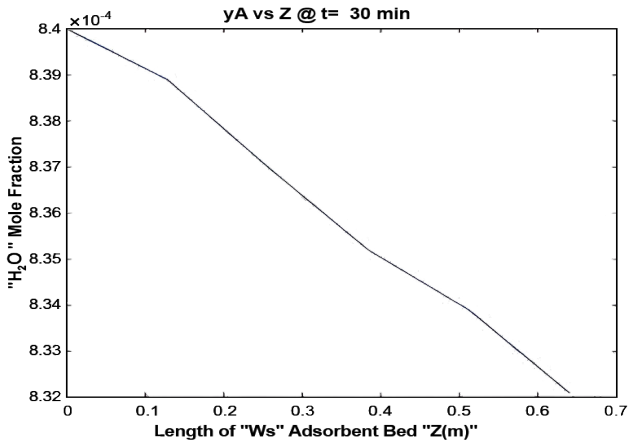

Figure 10. The Molar Fraction of Water Vapor along the Length of the Silica Gel bed Ws in the LAST Model

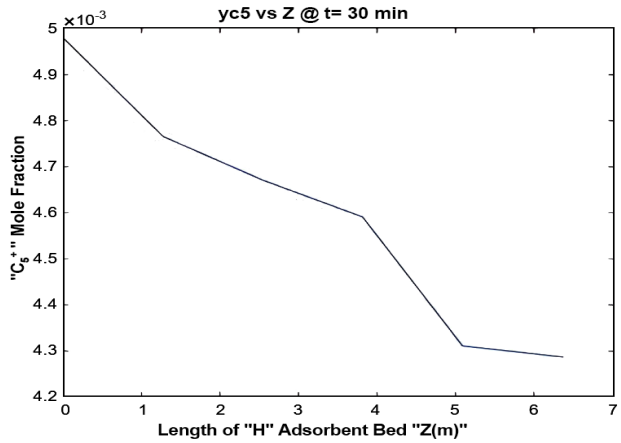

Figure 11. C_5^+ Mole Fraction along the Length of Silica Gel bed H in IAST Model

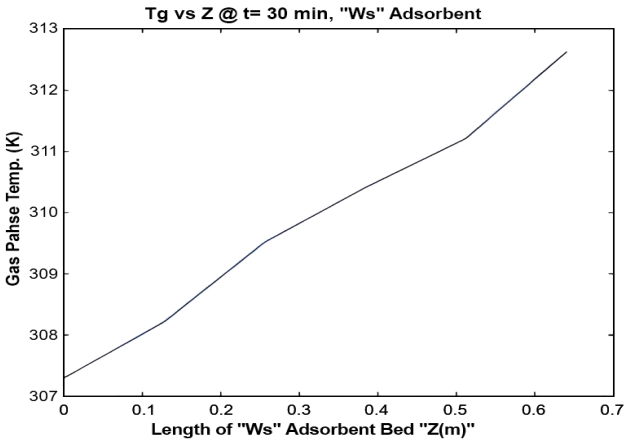

Figure 12. The Temperature of the Gas Phase along the Length of the Silica Gel bed Ws in the IAST Model

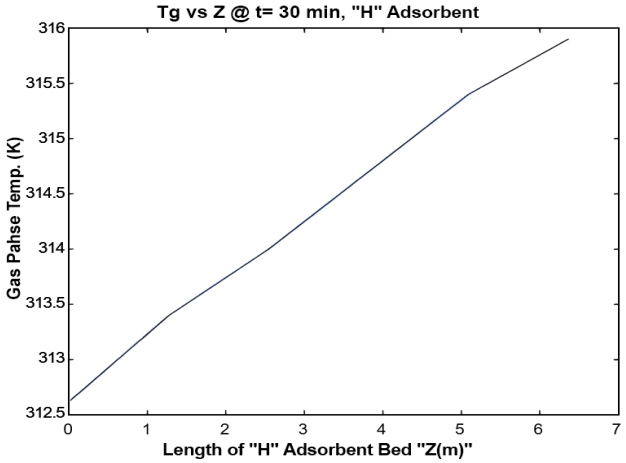

Figure 13. Gas-phase Temperature along the Length of the Silica Gel bed H in the IAST Model

5along the length of the bed filled with silica gel H within 30 min after the start of the

process. C_5^+ molecules are adsorbed by H silica gel during the bed and their concentration decreases. The output mole fraction of C_5^+ molecules is far from the actual data from the refinery, and this indicates the inadequacy of this isotherm in this system.

According to the above graphs (Figures 12 & 13) and the fact that the surface adsorption process is exothermic and also considering the outer surface of the filled bed as insulation, the gas temperature will be increased along the bed. This temperature increasing process is more intense in the early stages of the bed length due to more surface adsorption, due to the large concentration difference in the gas and solid phases. Therefore, by passing through the final stages of the substrate, the temperature increase is reduced. Based on the outputs of the IAST isotherm model, there is a big difference between the data obtained from the model and the actual data of the refinery, which indicates that the IAST isotherm is not suitable for the above system.

Due to the instability of adsorption process, the amount of adsorption of water and C_5^+ molecules were checked in four time periods for better evaluation and the results can be seen in the (Figures. 14 & 15). According to the results of the figures, the adsorption process is more in the early times due to the concentration potential difference in the solid and gas phase (unsaturation of silica gel from absorbable molecules). Over time, based on the saturation of solid phase, the adsorption process progresses slowly and the filled tower must enter the regeneration stage. According to the diagrams, the IAST isotherm has a high error in accurate and appropriate evaluation in the above system, and the output results differ greatly from the real data.

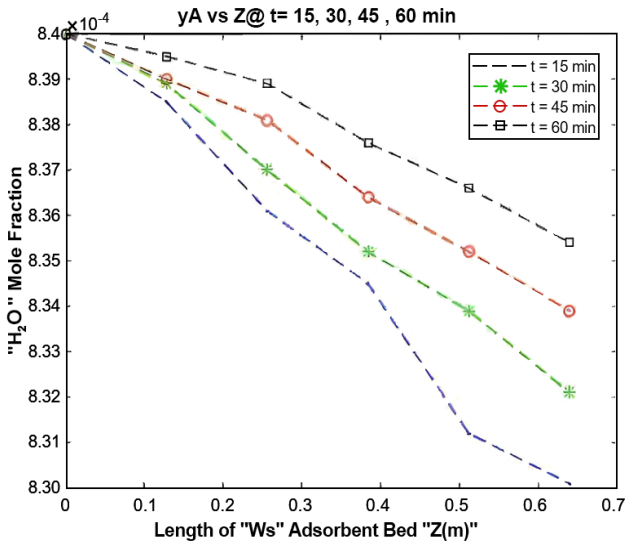

Figure 14. The Molar Fraction of Water Vapor along the Length of Silica Gel bed Ws in the IAST Model in Four Time Periods

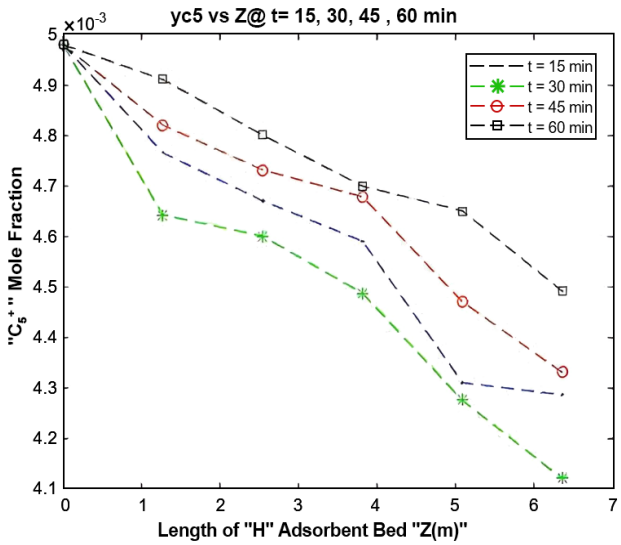

Figure 15. C_5^+ Mole Fraction along the Length of Silica Gel bed H in IAST Model in Four-time Intervals

According to the results in (Figures 16 & 17), the temperature of the gas fluid experiences a lower temperature increase over time along the bed, and the reason is based on what was explained earlier, the high concentration potential difference in the initial times and also, over time, the adsorbent bed becomes saturated with the desired molecule. As can be seen from the (Figure 16), the IAST isotherm has a high error in accurate and appropriate evaluation in the above system, and the output results differ greatly from the real data.

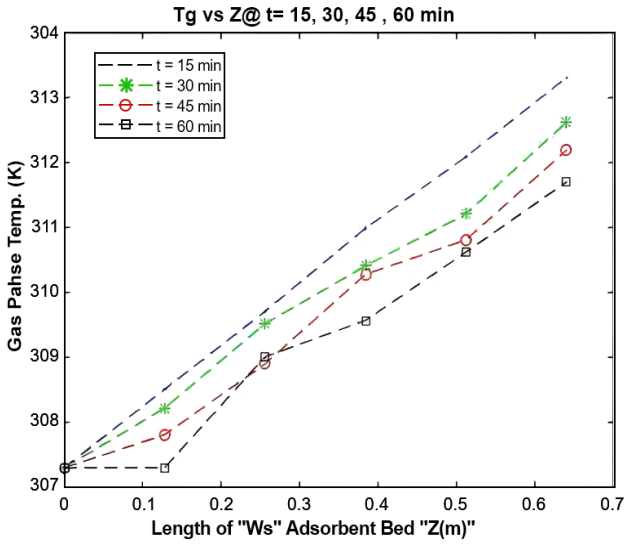

Figure 16. The Temperature of the Gas Phase along the Length of the Silica Gel bed *Ws* in the IAST Model at Four Time Intervals

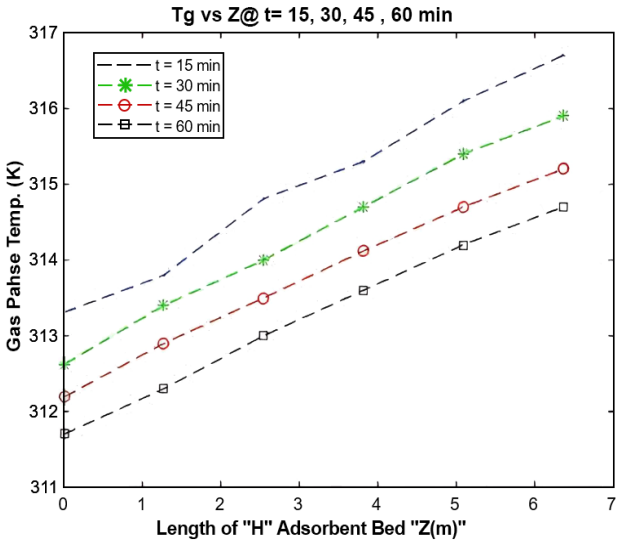

Figure 17. Gas-phase Temperature along the Length of the Silica Gel bed *H* in the IAST Model at Four Time Intervals

3.12. Comparing the Simulation Results of Langmuir Isotherm Model and IAST

According to the carried out simulations in the initial study case, for a better comparison of the results of using two Langmuir and IAST isotherm models in modeling the entire system of the adsorption process, the results of the output data from the adsorption towers and their difference with the real data, concretely, are given in the (Tables 7 & 8). According to the tables, the error rate of the IAST adsorption isotherm model for modeling the surface adsorption process in silica gel adsorbent is very high. Therefore, this is not suitable for the gas flare recovery system, sweetening and dehumidification using Nano adsorbents. In contrast, Langmuir isotherm model showed just an little error (less than 5%) in the three investigated parameters. This shows that for modeling and simulating the recovery process of gas flare by Nano adsorbents the Langmuir model is more suitable for adsorption on the surface of the adsorbent.

Table 7. The Comparison of Simulation Results of Two Isotherm Models Used

Row	Characteristic	The amount of input to the adsorp-tion unit	The amount of output from the adsorption unit (real data)	The amount of output from the adsorption unit (Simulation results) "Langmuir model"	The amount of output from the adsorption unit (Simulation results) "IAST Model"
1	Gas temperature	34.3 ℃	37 ℃	38.2 ℃	42.9 ℃
2	The mole fraction of water in the gas phase (Y_A)	0.00084	0.0008	0.0008074	0.0008321
3	C_5^+ molar fraction in the gas phase (Y_C)	0.00498	0.0030	0.003154	0.004287

Table 8. The Comparison of Simulation Results of Two Isotherm Models Used

Row	Characteristic	Some errors from the simulation "Langmuir model"	Some errors from the simulation "IAST Model"
1	Gas temperature	3.24%	15.94%
2	The mole fraction of water in the gas phase (Y_A)	0.92%	4.01%
3	C_5^+ molar fraction in the gas phase (Y_C)	5.13%	42.9%

3.13. The Simulation of the Second Part (Secondary Study Case)

In this section, the study case of the South Pars Phase 12 Gas Refinery is used. According to the investigations in the previous section, Langmuir isotherm was chosen as the most appropriate isotherm model for adsorption systems. Considering that the goal of this project is to recover gas flare by sweetening and its returning to the consumption line, three beds filled with nonadsorbent were selected to remove water vapor, heavy hydrocarbons and carbon dioxide. The dehumidifica-tion bed with *Ws* silica gel, heavy hydrocarbon removal bed with H-type silica gel, and carbon di-oxide removal bed with 4 *Å* molecular sieve adsorbent were considered. The used modeling in all three platforms was similar to the presented modeling in the previous sections, with the same boundary conditions and assumptions. In the simulation, the initial length of each bed was consid-ered to be 12 meters. According to the simulation in 4 time periods (similar to the simulation in the previous section), it is possible to obtain the optimal length for the bed in the best adsorption state for the South Pars Phase 12 refinery. On the other hand, due to the selection of 4 time periods in the simulated results, it is possible to obtain the appropriate and optimal time to start the regenera-tion process of each of the towers filled with adsorbent. In the following, the results of the simula-tion in the Matlab software environment are presented.

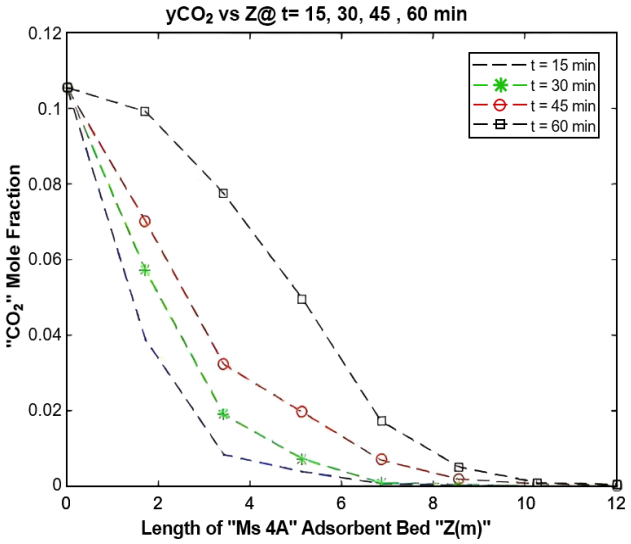

Figure 18. CO_2 Molar Fraction along the Length of the Ms-4A Silica Gel bed in the Langmuir Model for Four Time Periods

Due to the instability of the adsorption process, the amount of carbon dioxide adsorption was checked in four time periods for better evaluation and the results can be seen as shown in (Figure 18). According to the (Figure 18), the adsorption process is higher in the early times due to the concentration potential difference in solid and gas phase (unsaturation of silica gel from absorbable molecules). Over time, with the saturation of solid phase, the adsorption process progresses slowly and the filled tower must enter the regeneration stage. As it is clear from the graphs, the best time to move to the resuscitation stage is between 30 and 45 min. According to (Figure 19), in order to achieve an acceptable outlet concentration and in accordance with the experimental data of South Pars Refinery, the height of 11.1 meters

from the filled bed is the most optimal height to obtain the desired result in adsorption.

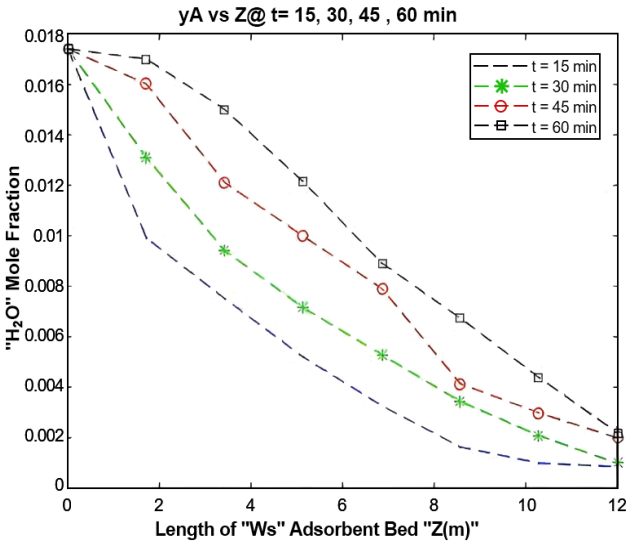

Figure 19. The Molar Fraction of Water Vapor along the Length of Silica Gel bed Ws in Langmuir Model in Four Time Intervals

Due to the instability of the adsorption process, the amount of water vapor adsorption was checked in four time periods for better evaluation and the results can be seen as shown in the (Figure 19). As can be understood from the (Figure 19), the adsorption process is higher in the early times due to the concentration potential difference in solid and gas phase (unsaturation of silica gel from absorbable molecules). Over time, based on the saturation of solid phase, the adsorption process progresses slowly and the filled tower must enter the regeneration stage. As can be seen from the above diagrams, the best time to move to the resuscitation stage is between 45 and 60 min. According to the above graphs, to achieve an acceptable outlet concentration and in accordance with the experimental data of the South Pars Refinery, the height of 10.5 meters from the filled bed is the most optimal height to obtain the desired result in adsorption. Due to the instability of the adsorption process, the amount of adsorption of heavy hydrocarbons was checked in four time periods for better evaluation, and the results can be seen as shown in the (Figure 20). According to (Figure 20), the adsorption process is higher in the early times due to the concentration potential difference in the solid and gas phases (unsaturation of silica gel from absorbable molecules). Over time, with the saturation of solid phase, the adsorption process decreases and the filled tower must enter the regeneration stage. As it is clear from the graphs, the best time to move to the resuscitation stage is between 45 and 60 min. According to the diagrams, in order to achieve an acceptable output concentration and in accordance with the experimental data of South Pars Refinery, a height of 10 meters from the filled bed is the most optimal height to obtain the desired result in adsorption.

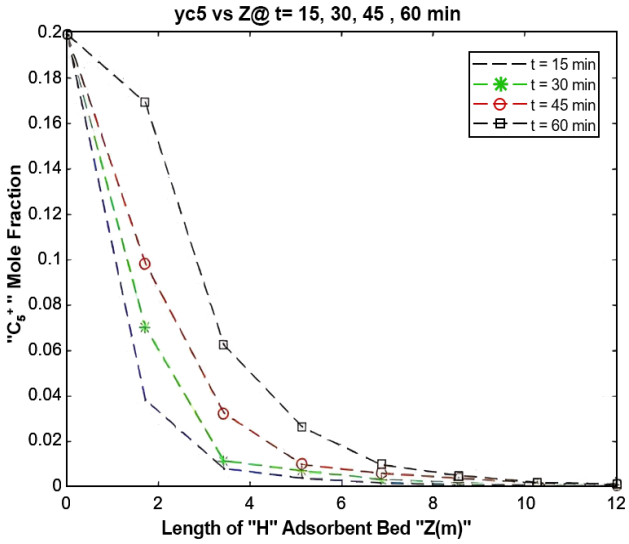

Figure 20. The Molar Fraction of Heavy Hydrocarbons along the Length of the Silica Gel bed H in the Langmuir Model in Four Time Periods

According to (Figure 20 & 21), as what was explained earlier, over the time, due to the high concentration potential difference in the early times and the saturation of the adsorbent bed over time of the desired molecule, the temperature of the gas fluid along the bed experiences a lower temperature rise. The temperature graphs for the other two substrates repeated a similar trend to the above trend. Therefore, we limited ourselves to only the above diagram for the substrate filled with a molecular sieve.

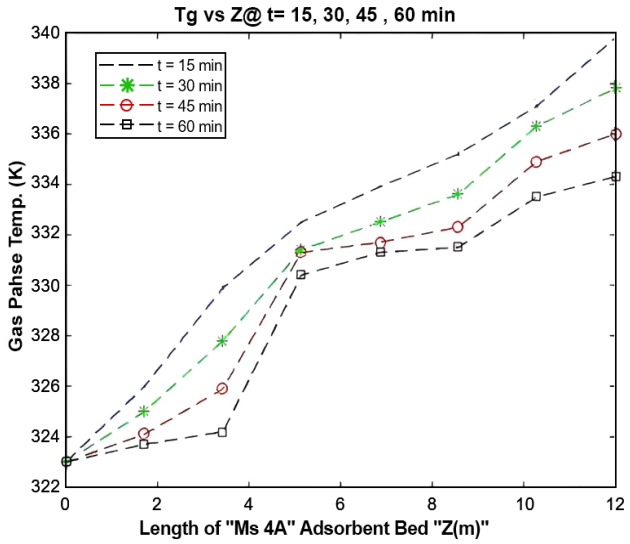

Figure 21. The Temperature of the Gas Phase along the Length of the Ms-4A Silica Gel bed in the Langmuir Model for Four Time Periods

3.14. Approximate Economic Evaluation

According to the carried out technical investigations in the previous sections, an economic evaluation is needed for a better analysis. In this way, by comparing the value of the gas flare price that is burned with the investment value in the construction and design of the adsorption unit to recover the gas flare, an approximate economic estimate is made. In this section, first, in the second study case (Phase 12 of South Pars), based on the amount of gas flow sent to the flare for burning, we estimate the dollar price of this flow. Also, the number of produced pollutants from this amount of flaring is calculated and reported. Then, based on the considered diagram for the adsorption unit, we calculate an approximate estimate of the fixed cost of the equipment, maintenance cost and etc.

3.15. Estimating the Price of Gas Flare and the Pollutants Caused by burning it

According to the reports of reliable authorities (Natural Gas Trading Economics), the current price of natural gas is 4.69 dollars per MMBtu. Every 1000 cubic meters of natural gas contains 36 MMBtu.

$$\frac{4.69\$}{1mmBtu}\times\frac{36mmBtu}{1000m^3}\times\frac{1m^3}{4.421Kg}\times\frac{76880Kg}{hr}=2936.02\,{}^{\$}/_{hr}=25.7\,{}^{m\$}/_{year}$$

According to the official and international rates of natural gas, the burning of natural gas sent to Flaring is 2936.02 dollars per hour and 25.7 million dollars per year, respectively.

3.16. The Amount of CO, NO_x Gas Emissions

In the desired gas refinery, steam-assistance flares are used, which in it steam employed to create smokeless combustion. Regarding to the high calorific value of the burned gases, the emission coefficients of the pollutants were selected and further with the help of the emission coefficients, the amount of emission of the pollutants can be calculated. The emission coefficients of NO_x and CO pollutants are presented in the (Table 9).

Table 9. Emission Coefficients of NOx and CO Pollutants in the Flaring System

Metal type	The calorific value of waste gas	NO_x (bm. $MMBtu^{-1}$)	CO (bm. $MMBtu^{-1}$)
(bm. MMBTU-1)	Top. >1000 BTU/Ft^3	0.0485	0.3503
Steam assist	Down. <1000 BTU/Ft^3	0.068	0.3465

3.17. Calculation of the Amount of Produced NO_x Pollutant

According to the calculation, the number of NO_x pollutants released from gas flaring is about 3000 tons per year.

$$(\frac{0.0485lb_{NO_x}}{MMBTU})\times(\frac{1270.77BTU}{SCF})\times(\frac{1MMBTU}{10^6BTU})\times(\frac{26.76\times10^6SCF}{1day})=1649.4\,{}^{lb_{NO_x}}/_{day}$$

$$(\frac{0.0485lb_{NO_x}}{MMBTU})\times(\frac{1270.77BTU}{SCF})\times(\frac{1MMBTU}{10^6BTU})\times(\frac{26.76\times10^6SCF}{1day})\times(\frac{1ton}{2000lb})\times(\frac{1000Kg}{1ton})=824.6\,{}^{Kg_{NO_x}}/_{day}$$

3.18. Calculation of CO Production Pollutant Amount

According to the calculation, the emission rate of carbon monoxide pollutants from gas flaring is about 2142 tons per year.

$$\left(\frac{0.35lb_{CO}}{MMBTU}\right)\times\left(\frac{1270.77BTU}{SCF}\right)\times\left(\frac{1MMBTU}{10^{6}BTU}\right)\times\left(\frac{26.76\times10^{6}SCF}{1day}\right)=11912.2\,{}^{lb_{CO}}\!/_{day}$$

$$\left(\frac{0.35lb_{CO}}{MMBTU}\right)\times\left(\frac{1270.77BTU}{SCF}\right)\times\left(\frac{1MMBTU}{10^{6}BTU}\right)\times\left(\frac{26.76\times10^{6}SCF}{1day}\right)\times\left(\frac{1ton}{2000lb}\right)\times\left(\frac{1000Kg}{1ton}\right)=5951\,{}^{Kg_{CO}}\!/_{day}$$

3.19. Approximate Economic Estimate of Setting Up an Adsorption Unit

According to the technical review and analysis of the flare gas recovery process using adsorbent towers, the economic estimation of this method helps to improve deciding for the faster use of flare gas recovery technology. In the economic evaluation of this study, some fixed costs (such as land, obtaining permits, etc.) and current costs (facility and utility costs, etc.) were considered for an approximate evaluation of 10% of the total fixed costs. First, in order to correct estimation of the adsorption process, an initial process map of the intended system is needed, which was designed by Microsoft Visio software (Figure 22).

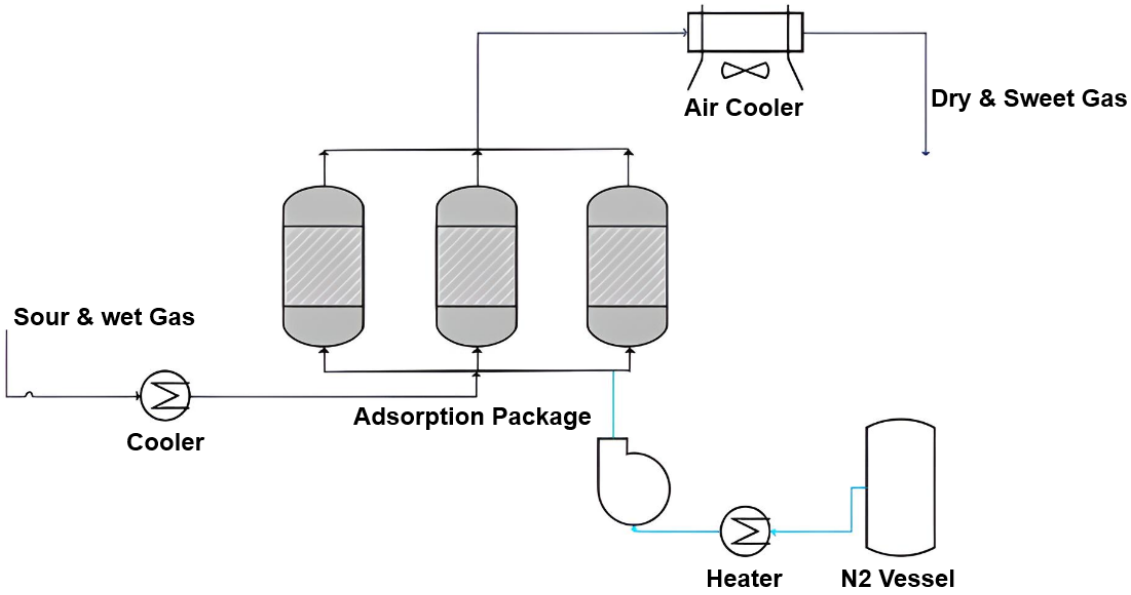

Figure 22. Schematic of the Adsorption Process in the Recovery of Gas Flares in South Pars Refinery

Due to the performed desired approximate comparison in the evaluation, the mentioned numbers in different references were employed. Thus, in some references, the cost of construction and maintenance of some equipment was in the form of curves with variable flow rates, which were extracted based on the mentioned gas flow rate in the previous sections (Voutchkov 2013). Some rotating equipment such as pumps, compressors, heat exchangers and air coolers were extracted from Aspen Hysys simulation software. Considering the above cases and assumptions, all the costs of equipment and maintenance and the method of using the absorber in the recovery of gas flare are given as follows.

Table 10. Estimated Costs of the Method of Using an Adsorbent to Recover Gas Flares in the South Pars Study Case

Row	Equipment	Fix Cost	Maintenance Cost
1	Inlet Cooler	458,000	68.700
2	Adsorbent Package	3*1650,000 4950,000	495,000
3	Air Cooler	300,000	45,000
4	N_2 Gas Vessel	510,000	76,500
5	N_2 Heater	210,000	21,000
6	N_2 Compressor	330,000	33,000
	Total Costs	6,300,000	739,200
	Total Fixed Costs of Equipment and Maintenance	7,039,200	
	Additional Costs (Such as Instruments, Permits, Piping)	703,920	
	The Total Approximate Cost of Project Implementation (the Dollar)	7,743,120	

To reach the decision point in the first phase of the study, simple payback period and simple rate of return (ROR) methods are usually used:

- Simple payback analysis
- Net present value
- A simple rate of return (Internal Rate of Return)

3.20. Simple Payback Analysis

This method is based on profitability criteria, and it is shown as a period of time that the total income related to the operation and installation of the facility after deducting all expenses, including taxes, is equivalent to the amount of investment required for consultation, purchase, and construction of the facility. This amount is equal to the ratio of the initial investment to the cash flow of annual earnings in the capital recovery period. In other words, it means:

$$\frac{\text{initial investment}}{\text{Annual savings}}$$

3.21. Net Present Value

In this method, all future incomes and expenses are converted to present value and added together. The interest rate is used to value money at this time:

$$NPV = \sum_{i=1}^{n} \left(\frac{R_i - C_i}{(1+r)^n} - C_0\right)$$

3.22. Internal Rate of Return

This method considers both the expected magnitude and timing of the cash flows in each period of the project's life. The internal rate of return for any investment proposal is the discount rate that equates the present value of the cash flow of expected costs to the present value of the cash flow of expected income.

$$NPV = 0 = \sum_{i=1}^{i} \left(\frac{R_j - C_j}{(1+r)^n} + 10\right)$$

In other words, the internal rate of return is the rate that makes the net present value of the project equal to zero. Now, according to the interpolation method, the amount of IRR can be calculated. The following diagram shows how to draw this process:

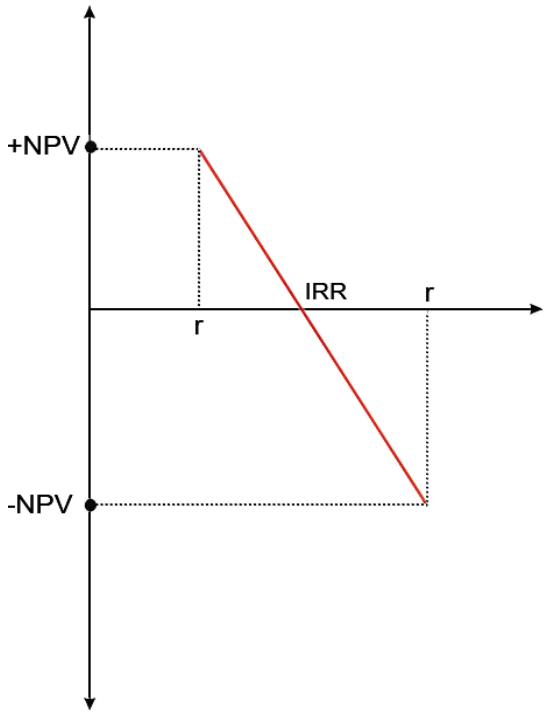

Figure 23. The Method for Drawing and Finding the IRR in the Graph

According to the chart, its formula is as follows, which can easily obtain the IRR amount.

$$IRR = [r_{low} + (r_{high} - r_{low})(\frac{NPV^{+}}{-NPV^{-} + NPV^{+}})] \times 100$$

In order to check this matter, it is always possible to achieve this by obtaining the investment cost, production rate, current cost, lifetime of the units, and annual profit of the project. The annual discount norm includes three factors:

- Inflation
- Interest rate
- Risk rate

This is not considered in these risk rate calculations. The (Table 11) shows the items calculated in the mentioned cases:

Table 11. Economic Evaluation of Gas Flare Recovery Methods

Unit Investment Cost	The Current Cost of the Unit	Unit Production Rate	The Amount of Profit Obtained from the Unit.	Return on Investment Period	NPV^{+}	IRR
The (Dollar)	The (Dollar)	M^3/hr	(Dollars/year)	(Year)	The (Dollar)	%
6.300.000	739.200	17389.7	25.700.000	3	459.750	13.141

4. Conclusion

One of the most important ways to prevent energy wastage is its management. According to the performed simulations related to the recovery method of gas flares, the output of each of the simulations, result in increase production and consequently decrease of environmental pollution. But the important point in this part is the economic evaluation and comparison of the flare gas recovery method with adsorbent towers filled with silica gel Ws, silica gel H and 4 $\mathring{A}$ molecular adsorbers, with considering the amount of pollution and the waste of capital in burning gas flare, which is very important in terms of an economic priority compared to the burning of gas sent to the flare. According to the performed economic evaluation, with the implementation of the flare gas recovery unit by absorber towers filled with nanoadsorbents, with an investment of approximately 25% of the cost of burned flare gas per year, within three years the entire cost returned and can to make the unit profitable. This is a reason for the recovery of the flare gas, on the other hand, it prevents much environmental pollution. In order to validation of derived results from modeling and simulation, actual operation data were used also.

Legend Caption

C_1	Water vapor concentration in gas phase
q_1	Vapor concentration in solid phase
Vp	The volume of the adsorbent beads in bed
Z	Length of bed
t	Time
K_A	Mass transfer coefficient
q_A^*	Equilibrium concentration in solid and gas phase interface.
d	Diameter of bed
P_A	Partial pressure of gas
P_t	Total pressure of gas
C_{pg}	Average heat capacity of gas balk
h_w	Convection heat transfer coefficient between gas balk and internal surface of bed side
C_{ps}	Average heat capacity of solid phase
h_p	Convection heat transfer coefficient between gas balk and adsorbent particles
ΔH	Exchanged heat in adsorbent process
ε	Porosity of bed
T_0	Base temperature
T_w	Temperature of side bed
T_f	Temperature of fluid phase
T_s	Temperature of solid particles
ρ_g	Density of gas phase
ρ_s	Density of solid phase
λ_L	Axial heat transfer coefficient

References

A. Ahsan, H. Ahsan, J. S. Olfert, L. W. Kostiuk. Experimental Thermal and Fluid Science 2019, 103, 133-142.

A. A. Tofigh, M. Abedian. Renewable and Sustainable Energy Reviews 2016, 57, 1296-1306.

M. Jafari, S. Ashtab, A. Behroozsarand, K. Ghasemzadeh, D. A. Wood. Gas Processing Journal 2018, 6, 1-20.

A. A. Keshavarz, the fourth national process engineering conference, refinement and petrochemical, 2015.

M. Jafari, A. Vatani, M. S. Deljoo, A. Khalili-Garakani. Journal of Gas Technology 2021, 6, 28-44.

A. Hajizadeh, M. Mohamadi-Baghmolaei, R. Azin, S. Osfouri, I. Heydari. Chemical Engineering Research and Design 2018, 131, 506-519.

H. Freundlich, H. Hatfield. Ltd., London 1926, 110-114

E. Barekat-Rezaei, M. Farzaneh-Gord, A. Arjomand, M. Jannatabadi, M. H. Ahmadi, W.-M. Yan.

K. Fard, M. Shafiee. Adv. J. Chem. A 2019, 3, 49-57.

A. Hajizadeh, M. Mohamadi-Baghmolaei, R. Azin, S. Osfouri, I. Heydari. Chemical Engineering Research and Design 2018, 131, 506-519.

M. Heidari, A. Ataei, M. H. Rahdar. Applied Thermal Engineering 2016, 104, 687-696.

E. L. Ng, J. Honeysett, Y. Scorgie. Sustainable Production and Consumption 2023, 35, 116-128.

F. G. U. Strategy. The International Bank for Reconstruction and Development. The World Bank 2004, 113.

M. Khanipour, A. Mirvakili, A. Bakhtyari, M. Farniaei, M. R. Rahimpour. Fuel Processing Technology 2017, 166, 186-201.

M. Zolfaghari, V. Pirouzfar, H. Sakhaeinia. Energy 2017, 124, 481-491.

M. Davoudi, M. Rahimpour, S. Jokar, F. Nikbakht, H. Abbasfard. Journal of Natural Gas Science and Engineering 2013, 13, 7-19.

M. Gholami, M. Talaie. Industrial & engineering chemistry research 2010, 49, 838-846.

M. Saidi. International Journal of Hydrogen Energy 2018, 43, 14834-14847.

M. R. Rahimpour, S. M. Jokar. Journal of hazardous materials 2012, 209, 204-217.

1. E. N. Ojijiagwo, C. F. Oduoza, N. Emekwuru. Procedia Manufacturing 2018, 17, 444-451.

M. Xue, X. Li, X. Cui, X. Cheng, S. Liu, W. Xu, Y. Wang. SPE Prod. Oper 2023, 49, 504-512.

M. Jafari, A.Vatani, MS. Deljoo, A. Khalili-Garakani, Journal of Gas Technology. 2021, 6, 28-44.

M. M. Sabaghian, M. Hajipour. Journal of Gas Technology. 2022, 7, 4-15.

شبیه‌سازی و ارزیابی اقتصادی بازیافت گاز مشعل با استفاده از نانوجاذب‌ها

- میثم بیژنی خو[1]، زهره سعادتی[2*]، افسانه ملکی[2]

۱. دانشجوی دکتری، گروه شیمی، واحد امیدیه، دانشگاه آزاد اسلامی، امیدیه، ایران

۲. دانشیار، گروه شیمی، واحد امیدیه، دانشگاه آزاد اسلامی، امیدیه، ایران

(ایمیل نویسنده مسئول: zo.saadati@iau.ac.ir)

چکیـــــــده

صنعت نفت و گاز با انتشار روزافزون گازهای مشعل که ناشی از گسترش جهانی صنعت و افزایش مصرف سوخت فسیلی در پالایشگاه‌ها و کارخانه‌های پتروشیمی است، با چالشی حیاتی مواجه است. اثرات زیست محیطی قابل توجه این انتشار گازهای مشعل، نیاز مبرمی به توسعه استراتژی‌های مؤثر برای به حداقل رساندن خطرات زیست محیطی مرتبط ایجاد کرده است. با این حال، پیاده‌سازی فن‌آوری‌هایی برای کاهش انتشار گازهای مشعل، موانع اقتصادی و زیست‌محیطی را به همراه دارد. در این مطالعه، ما کاربرد نانوجاذب‌ها را در برج‌های آکنده به‌عنوان یک رویکرد امیدوارکننده برای بازیابی و استفاده مجدد از گازهای مشعل بررسی کردیم. با استفاده از نرم‌افزار MATLAB، دو مطالعه موردی را برای ارزیابی عملکرد جاذب‌های مختلف، از جمله ژل‌های سیلیکا Ws، H و همچنین یک غربال مولکولی $4\mathring{A}$، برای بازیابی و تبدیل گازهای مشعل ترش به گاز شیرین و مرطوب انجام دادیم. تجزیه و تحلیل نشان داد که مدل ایزوترم لانگمویر مناسب‌ترین نتایج شبیه‌سازی را ارائه می‌کند که امکان‌سنجی فنی و اثربخشی این رویکرد را نشان می‌دهد..

واژگان کلیدی: جاذب، ژل سیلیکا، غربال مولکولی، شبیه‌سازی مشعل، گاز طبیعی